Quantification Studies in Continuous-Flow ^{13}C Nuclear Magnetic Resonance Spectroscopy by Use of Immobilized Paramagnetic Relaxation Agents

Holger H. Fischer,[†] Michael Seiler,[‡] Thomas S. Ertl,[‡] Ulrich Eberhardinger,[‡] Helmut Bertagnolli,[‡] Heribert Schmitt-Willich,[§] and Klaus Albert*[,†]

Institut für Organische Chemie, Auf der Morgenstelle 18, 72076 Tübingen, Germany, Institut für Physikalische Chemie, Pfaffenwaldring 55, 70550 Stuttgart, Germany, and Schering AG, 13342 Berlin, Germany

Received: July 16, 2002

Different types of immobilized free radicals as well as immobilized paramagnetic gadolinium(III) complexes were synthesized and used as relaxation agents to shorten the spin−lattice relaxation times T_1 of analytes in quantitative *continuous-flow* ^{13}C nuclear magnetic resonance spectroscopy (NMR). The immobilized paramagnetic relaxation agents were characterized with electron paramagnetic resonance spectroscopy (EPR) and extended X-ray absorption fine structure spectroscopy (EXAFS). With these types of paramagnetic relaxation agents, it was possible to obtain a 4-fold increase in signal-to-noise ratio per unit time, and an almost quantitative NMR spectra in continuous-flow ^{13}C NMR spectroscopy could be acquired with this method.

Introduction

The direct on-line coupling of high-performance liquid chromatography (HPLC) with high-field ^{1}H NMR spectroscopy is an established hyphenated technique and one of the more powerful tools for structure elucidation.[1,2] Herein, the use of *continuous-flow* ^{13}C NMR spectroscopy is quiet uncommon due to the low gyromagnetic ratio and the low natural abundance of ^{13}C nuclei. Despite these facts, the investigation of complex reaction processes with ^{13}C NMR spectroscopy provides often more information than ^{1}H NMR spectroscopy owing to its much higher spectral dispersion (∼220 ppm). Continuous-flow ^{13}C NMR spectroscopy has been applied for the investigation of reaction intermediates,[3] electrochemical reactions,[4] and in vivo metabolism.[5] None of these studies achieved a high degree of quantification. However, for structural elucidation and many other applications, a better quantification of ^{13}C NMR spectra would be very helpful.

For conventional ^{13}C NMR spectra some methods for improved quantification have been known for many years. Chromium tris(acetylacetonate) ($Cr(acac)_3$) is often used to shorten long spin−lattice relaxation times and to eliminate the nuclear Overhauser effect (NOE) in proton-decoupled ^{13}C NMR spectra.[6−10] Problems with the $Cr(acac)_3$ method, however, have been reported for larger molecules.[11] Inverse-gated decoupling can also be employed as a general method for eliminating the NOE effect.[12,13] In this method, the decoupler is gated on during acquisition and off during the recovery time. The pulse repetition time, which consists of the acquisition time AQ and the relaxation delay D1, is adjusted to at least 3−5 times the T_1 time of the slowest relaxing carbon atom. Several applications for the quantitative analysis of molecule mixtures as well as optimization steps using conventional ^{13}C NMR spectroscopy have been reported.[12,14,15]

The first quantitative application of continuous-flow ^{13}C NMR spectroscopy was done by Laude and Wilkins,[16] followed by several other reports.[17,18] Quantification in these cases was performed by inserting a premagnetization tubing with a volume up to 30 mL upstream of the NMR probe. But premagnetization volumes of this size would lead to significant band broadening in HPLC NMR coupling experiments.[19] Bruck and Fyfe[20] used immobilized free radicals (IFR) for the reduction of the premagnetization volume in continuous-flow NMR experiments without the line broadening that would accompany direct addition of relaxation agents. Wilkins[21] and later Laude[22] repeated the technique in superconducting magnets and showed the potential of IFRs for quantitative ^{13}C NMR spectroscopy. In the present study, IFRs and new immobilized paramagnetic relaxation agents, Gd(III) complexes, are investigated. Paramagnetic metal complexes have long been used as water proton relaxation agents, including for magnetic resonance imaging (MRI).[23,24] Here the Gd^{3+} ion as paramagnetic central atom is preferred, due to its very efficient relaxation effect. This is caused by the total symmetric arrangement of seven unpaired electrons in the 4f shell of Gd^{3+} resulting in a large magnetic moment and a favorably slow electronic relaxation rate.[25] Multifrequency EPR[26] and NMR[27−29] studies on structure, exchange dynamics, relaxometry, as well as temperature and pH dependence have been done with the free Gd^{3+} ion and with the free chelated, which means nonimmobilized, Gd(III) complexes.

Extended X-ray absorption fine structure (EXAFS) spectroscopy has been considered to be a powerful technique for determining the local atomic environment of a specific atom without regard to the state of the sample. An analysis of the EXAFS spectrum provides information on the bond distance, the coordination number, the "Debye−Waller" factor, and the nature of the scattering atoms surrounding an excited atom.[30,31] In contrast to X-ray diffraction, it is possible to study amorphous solids with this method. It is the objective to investigate the

* To whom correspondence should be addressed. Institut für Organische Chemie, Universität Tübingen, Auf der Morgenstelle 18, 72076 Tübingen, Germany. E-mail: klaus.albert@uni-tuebingen.de. WWW: http:www.uni-tuebingen.de/uni/cok.

[†] Institut für Organische Chemie.

[‡] Institut für Physikalische Chemie.

[§] Schering AG.

10.1021/jp021631d CCC: $25.00
Published on Web 04/29/2003

local structure around the central Gd atom for the first two atom shells to clarify the influence of the polymer as carrier material. This can be achieved by the comparison of the interatomic distances of the local structure around the central Gd atom of both the nonfixed Gd(III) complexes and the complexes fixed on silica.

In this paper the advantage of IFRs and Gd(III) complexes in increasing the signal-per-noise ratio in continuous-flow ^{13}C NMR is shown and compared with conventional continuous-flow ^{13}C NMR spectroscopy.

Theory

Problems arise in the interpretation of continuous-flow ^{13}C NMR spectra when spin−lattice relaxation times T_1 are long or deviate greatly for different nuclei, e.g., for quaternary or aromatic carbon atoms. In this case, the full relaxation of all nuclei is not possible to achieve in an acceptable time, even if pulse angles of less than 90° are used. Consequently, interpretation and quantification become difficult or even impossible.

The spin−lattice relaxation time T_1 as well as the spin's relaxation time T_2 in flowing systems depend on the residence time τ of the sample in the detection volume V_D and the flow rate u. Equations 1 and 2 describe the relationships.[3]

$$\frac{1}{T_{i_{flow}}} = \frac{1}{T_{i_{static}}} + \frac{1}{\tau} \tag{1}$$

$$\tau = V_D/u \tag{2}$$

When the flow rate is increased such that the residence time of the sample in the detection volume is equal to the repetition time of the FID, a 90° pulse angle can be used independent of the T_1 relaxation time for several nuclei.[32]

However, to achieve the Boltzmann distribution it is necessary that the nuclei remain for a time 3−5 times larger than T_1 in the magnetic field. This requirement leads to very large premagnetization volumes for higher flow rates.[16,17,33]

It is possible to reduce the premagnetization volume by manipulating the spin−lattice relaxation times of sample nuclei. This is accomplished by adding stable free radicals or other paramagnetic relaxation agents, such as Gd(III) complexes, to the solution. However, the spin's relaxation time T_2 is also affected, and therefore, extensive line broadening is observed where little or no resolution is achieved. In addition, the sample is polluted with a relaxation agent. For better results, the research groups of Fyfe,[20] Dorn,[34] and Laude[22] have immobilized radicals in the premagnetization volume by surface modification of silica gel or polymer beads. This immobilization leads to a reduction of the T_1 times in the premagnetization volume by a factor of up to 100 and has no decreasing effect on the T_2 times.

Dorn et al. have used these IFRs to transfer magnetization from electron to nuclear spins by saturation of the EPR frequencies of the radicals.[35−41] This so-called dynamic nuclear polarization (DNP) promises a theoretical gain in sensitivity by a factor of 660 for ^1H nuclei and 2660 for ^{13}C nuclei.[42]

Experimental Section

Synthesis. Free radicals as well as paramagnetic Gd(III) complexes were immobilized on silica gel by classic surface modification procedures. The structures are shown in Figure 1.

For APS−TEMPO, silica gel (ProntoSIL 60, 25−40 μm, 500 Å; Bischoff, Leonberg, Germany) was modified with triethoxy-3-aminopropyl-silane via the bake reaction of Buszewski.[43] In a second step, the carboxy-functionalized TEMPO radical

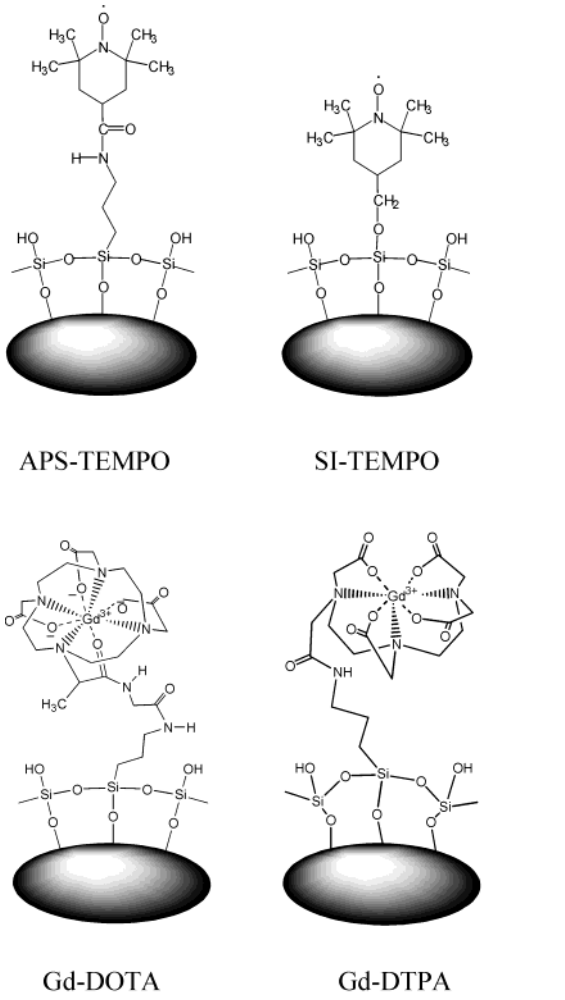

Figure 1. Structures of immobilized free radicals and paramagnetic Gd(III) complexes.

(2,2,6,6-tetramethylpiperidinoxyl) (Aldrich, Steinheim, Germany) was bounded to the free amino group of the aminopropyl modified silica gel by the aid of coupling auxiliary reagents hydroxybenzotriazole (HOBt) and diisopropylcarbodiimide (DICI) (both from Aldrich, Steinheim, Germany). SI−TEMPO was yielded in a two-step procedure by modifying silica gel with dichlorodimethylsilane, followed by TEMPOL, (4-hydroxy-2,2,6,6-tetramethyl-piperidinoxyl) (Aldrich, Milwaukee, WI) in anhydrous toluene. The products were washed several times with toluene, dichloromethane, methanol, and water, respectively. The yielded immobilized radicals are called silica phase immobilized nitroxides (SPIN).

Paramagnetic Gd(III) ions were complexed with modified 1,4,7,10-tetraazacyclododecane *N*,*N*′,*N*′,*N*‴-tetraacetic acid (DOTA) as well as with diethylentriamine *N*,*N*,*N*′,*N*″,*N*″-pentaacetic acid (DTPA) and were immobilized on aminopropyl modified silica gel via the known coupling reactions mentioned above.

Subsequently, the products were packed in columns and were continuously rinsed in a recycled-flow system with methanol and ethylbenzene, respectively, to remove unreacted reagents.

Apparatus. The apparatus used for continuous-flow ^{13}C NMR experiments is shown in Figure 2.

The analyte was pumped in a recycled-flow system through the NMR flow probe by a HPLC pump (Bischoff Chromatography, Leonberg, Germany). Stainless steel capillaries were used as transfer lines to connect pump and NMR flow probe.

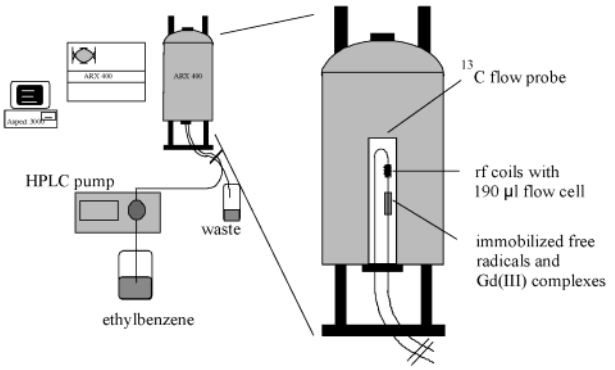

Figure 2. Setup for the continuous-flow ^{13}C NMR experiments, with positions for the immobilized free radicals, the paramagnetic Gd(III) complexes, and the dummy column, respectively.

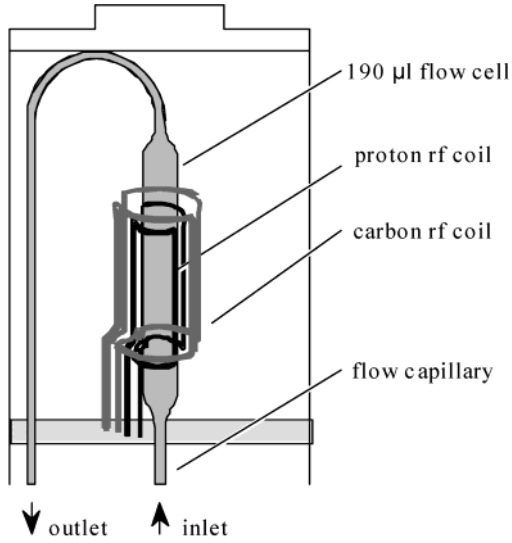

Figure 3. Continuous-flow ^{13}C NMR probe with 190 μl detection cell.

Detection was carried out with a HP 1050 variable-wavelength UV detector (Hewlett-Packard, Waldbronn, Germany), which was equipped with a high-pressure flow cell. The flow probe used for NMR detection is shown in Figure 3. The flow cell consists of a 5 mm glass tube giving a NMR-active cell volume of 190 μL. The ARX 400 NMR spectrometer (Bruker, Rheinstetten, Germany) was controlled by an O2 workstation (SGI, USA) computer system.

Method. The relationship between signal-to-noise ratio and flow rate was observed for continuous-flow ^{13}C NMR spectroscopy with a premagnetization volume of 25 mL. For this, spectra of a solution of 0.1 M cholesterol acetate in $CDCl_3$ were recorded under *stopped-flow* conditions as well as 12 times at various flow rates ranging from 1 to 20 mL/min.

For the experiments with relaxation agents, the different paramagnetic phases, packed in small PEEK columns, were inserted into the flow path of the continuous-flow ^{13}C NMR probe. The columns were positioned in the premagnetization volume of the flow NMR probe approximately 7 cm below the radio frequency detection coil (see Figure 2).

For reference measurements, one column was packed with aminopropyl-modified silica gel only: this will be called from now on the "dummy column".

All NMR spectra were recorded in the inverse-gated decoupling mode. Relaxation delay was adjusted each time to the actual residence time τ which corresponds to the flow rate.

For the flow experiment with cholesterol acetate, the number of scans recorded for the 12 spectra was held constant at 128.

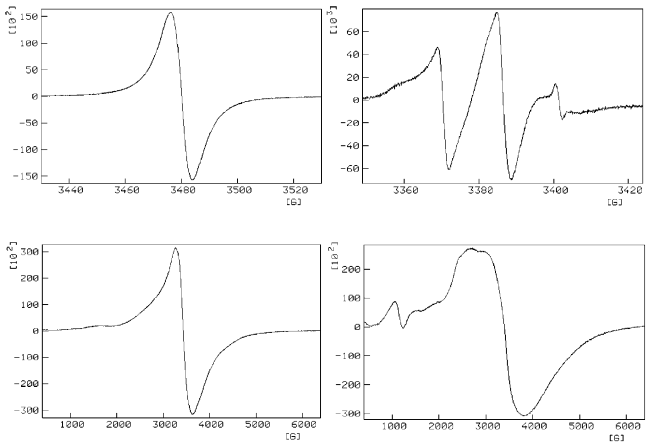

Figure 4. EPR spectra of APS−TEMPO (a), SI−TEMPO (b), Gd−DOTA (c), and Gd−DTPA (d).

In all experiments with paramagnetic relaxation agents, neat ethylbenzene was used as analyte and recorded under stop-flow conditions as well as at 12 different flow rates ranging from 0.01 to 20.00 mL/min. One transient per spectrum with a total of 32k data points and a spectral width of 18520 Hz were acquired, resulting in an acquisition time of 0.885 s. In all transients a flip angle of 90° (7.4 μs) was used. The integral values of all ethylbenzene spectra were calibrated to the methyl group of each spectrum.

Results and Discussion

Figure 4 depicts the EPR spectra of two silica phase-immobilized TEMPO radicals (SPINs), APS−TEMPO (a) and SI−TEMPO (b), as well as two silica phase-immobilized Gd-(III) complexes, Gd−DOTA (c) and Gd−DTPA (d). Due to the high loading of silica beads with TEMPO with approximately 10^{18} spins/g, the triplet of APS−TEMPO, such as that in the spectrum of SI−TEMPO with a TEMPO loading of 10^{17} spins/g, is no longer resolvable. This is caused by the increased intramolecular electron−electron exchange. The line width of the single line and central line, respectively, is 18 G for APS−TEMPO and 2.4 G for SI−TEMPO. Gd−DOTA is loaded with 3.47 wt % Gd. The EPR spectra of Gd−DOTA shows a single line with a g factor of 1.98 and a line width of 400 G. Seven unpaired electrons of Gd^{3+} ($6s^05d^04f^7$ configuration of Gd^{3+}) result in a dramatically reduced electron spin spin relaxation time T_2. Gd−DTPA is loaded with 2.94 wt % Gd. The spectrum of Gd−DTPA depicts a similar broad central line but interrupted by a fine structure. Measurements at deep temperatures (77 K) as well as measurements in ethanol and chloroform suspensions did not lead to a significant change in resolution; therefore, influences of spacer length and solvent effects on the line width can be neglected.

The EXAFS measurements of all Gd(III) complexes were performed at the Gd-L_3-edge (E_{L3} = 7243 eV) with the beam line ×1.1 of the Hamburger Synchrotronstrahlungslabor (HASYLAB) at DESY, Hamburg, at 20 °C, with a Si(111) double-crystal monochromator under ambient conditions (5.46 GeV, beam current 98 mA). Data were collected in transmission mode with ion chambers. Energy calibration was monitored with 20 μm thick Gd metal foil at the L_3-edge (E_{L3} = 7243 eV). All measurements were performed under an inert gas atmosphere. The samples were prepared as pellets of a mixture of complexes **1**−**4** and polyethylene. Data were analyzed with a program package specially developed for the requirements of amorphous samples.[44] The program AUTOBK of the University of Wash-

TABLE 1: EXAFS-Determined Structural Data of the Gd−DOTA Complexes[c]

	free Gd−DOTA (1)			immobilized Gd−DOTA (3)		
	N	*r*, Å	*σ*, Å	*N*	*r*, Å	*σ*, Å
Gd−(O_1)	4.1 ± 0.6	2.32 ± 0.02	0.063 ± 0.009	5.1 ± 0.7	2.33 ± 0.02	0.087 ± 0.013
Gd−(O_2)	5.1 ± 0.7	2.48 ± 0.02	0.071 ± 0.011	5.2 ± 0.7	2.45 ± 0.02	0.112 ± 0.017
Gd−(N_1)	4.3 ± 0.6	2.69 ± 0.03	0.059 ± 0.009	4.3 ± 0.6	2.65 ± 0.03	0.081 ± 0.012

[c] Coordination number *N*, absorber-backscatterer distance *r*, and Debye−Waller factor *σ* with calculated standard deviations. The letters in parentheses refer to the Gd−DOTA complexes (see Figure 5) and indicate the molecule where the backscattering atom is located.

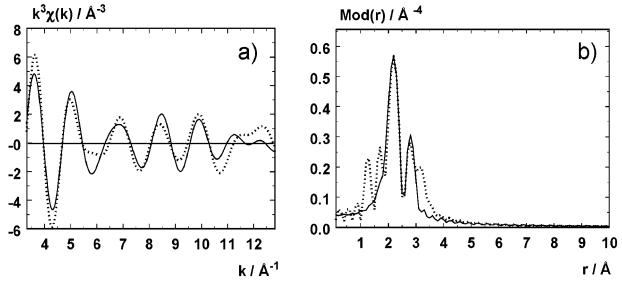

Figure 5. Experimental (dotted line) and calculated (solid line) $k^3\chi$ (k) functions (a) (k range: 3.31−12.82 Å^{-1}) and their Fourier transforms (b) for the free Gd−DOTA complex (Gd-L_3-edge) (see Table 1 for fit parameter).

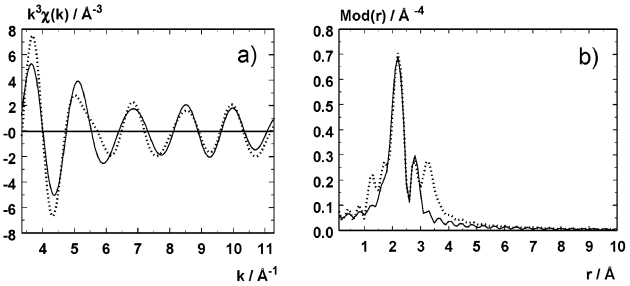

Figure 6. Experimental (dotted line) and calculated (solid line) $k^3\chi$ (k) functions (a) (k range: 3.34−11.29 Å^{-1}) and their Fourier transforms (b) for the immobilized Gd−DOTA complex (Gd-L_3-edge) (see Table 1 for fit parameter).

ington[45] was used for the background removal, and the program EXCURV92[46] was used for the evaluation of the XAFS function. The resulting EXAFS function was weighted with k^3. Data analysis in k space was performed according to the curved-wave multiple-scattering formalism of the program EXCURV92. The mean free path of the scattered electrons was calculated from the imaginary part of the potential (VPI was set to −4.00), the amplitude reduction factor AFAC was fixed at 0.8, and an overall energy shift ΔE_0 was introduced to fit the data. Optimized parameters were absorber−backscatterer distances, Debye−Waller factors, as well as coordination numbers. The adaptation of the coordination numbers was done to make an approach to the unsorted situation in noncrystalline environment, resulting in odd values (see Table 1, 2 for exact values), in contrast to the integer coordination numbers of crystalline samples.

In fitting the EXAFS functions (Figures 5a and 6a), the individual absorber−scatterer contributions were separated by Fourier filtering in the range of 1.0−3.0 Å. For the free Gd−DOTA complex (Figures 5 and 7a,) the presence of four equivalent gadolinium−oxygen bond distances at 2.32 Å and, for the free Gd−DTPA complex (Figure 6 and Figure 7b), five equivalent gadolinium−oxygen bond distances at 2.34 Å were identified.

Usually an inner-sphere water molecule with a significantly larger gadolinium−oxygen bond distance, in the range between 2.40 and 2.49 Å, is found by X-ray diffraction[47] in most Gd complexes. We determined five equivalent gadolinium−oxygen bond distances at 2.48 Å for Gd−DOTA and 2.49 Å for Gd−DTPA, respectively.

The second intense peak of the Fourier transform (Figures 5b and 8b) was matched to a nitrogen atom shell, surrounding the metal center with four equivalent gadolinium−nitrogen atomic distances at 2.69 Å. In the case of the free Gd−DTPA complex, we found three equivalent gadolinium−nitrogen atomic distances at 2.70 Å.

As follows from the analysis of the EXAFS-spectra of the immobilized Gd complexes (see Tables 1 and 2), the distances and the coordination number are not changed significantly by the fixation of the free Gd complexes on silica, except for the coordination number of the first shell. The comparison of the free and the immobilized Gd complexes shows that the number of coordinated oxygen (O_1) in both immobilized Gd complexes is increased by one and that the Gd−(O_1) distance is significantly shorter than the Gd−(O_2) distance of the inner-sphere water molecules in Gd hydrate.[47] For the corresponding free Gd complexes, it was impossible to find the same coordination numbers of oxygen atoms, as in the case of the immobilized Gd complexes, and thus the binding to an oxygen atom of the polymer seems to be possible, especially in the case of the immobilized Gd−DTPA complex. For the immobilized Gd−DOTA complex, there are two possibilities for the coordination of a fifth oxygen atom (O_1): on one hand, the coordination of an oxygen atom of the glycine linker to the DOTA complex and, on the other hand, the coordination of an oxygen atom of the polymer (see Figure 7c). With EXAFS spectroscopy it is not possible to distinguish here between these both structural suggestions, and thus, both postulated structures are probable in the case of the immobilized Gd−DOTA complex. The coordination number of the inner sphere water molecules and of the other ligands remains unaltered at a constant value for all investigated Gd complexes (see Tables 1 and 2).

The determined gadolinium−oxygen and gadolinium−nitrogen bond distances of free and immobilized Gd complexes (see Tables 1 and 2) are in good agreement with X-ray diffraction[47] and EXAFS[48] studies. Due to the close and equivalent positions, in agreement with the crystallographic and spectroscopic data of the oxygen and the nitrogen atoms surrounding the Gd center, a chemical bond of the oxygen and nitrogen atoms at the Gd center can be suggested in all investigated Gd complexes.

From the structural data of the Fourier transforms of the complexes, summarized in Tables 1 and 2, we can deduce the structures of the immobilized Gd complexes by a distorted tricapped trigonal prism in which the central Gd^{3+} ion has the characteristic coordination number of nine without consideration of the inner-sphere water molecules (Figure 7c,d).[24]

The relationship between signal-to-noise ratio and flow rate in conventional continuous-flow ^{13}C NMR spectroscopy is demonstrated in Figure 10, where 12 spectra of 0.1 M cholesterol acetate, recorded under continuous- and stopped-flow conditions in the inverse-gated decoupling mode, are

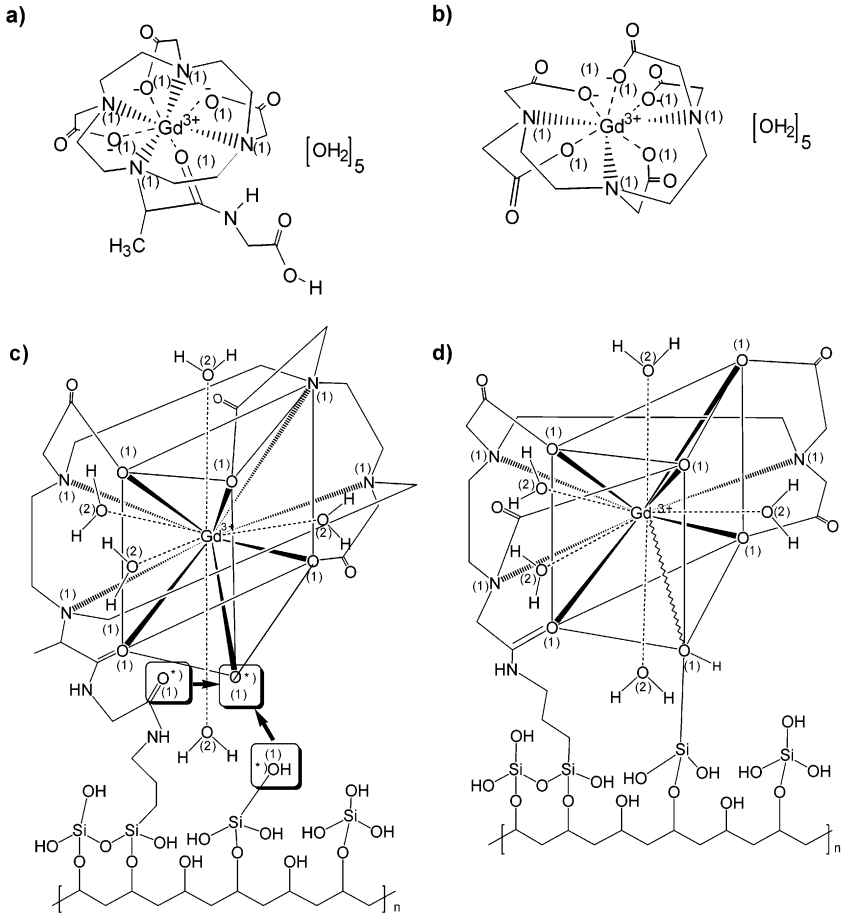

Figure 7. Postulated structures of the free Gd−DOTA (a) and free Gd−DTPA complex (b), and immobilized Gd−DOTA (c) and immobilized Gd−DTPA complex (d), fixed on silica. The oxygen atoms, marked by asterisk represents two possibilities of the coordination of oxygen at the Gd center (c).

TABLE 2: EXAFS-Determined Structural Data of the Gd−DTPA Complexes[c]

	free Gd−DTPA (2)			immobilized Gd−DTPA (4)		
	N	*r*, Å	*σ*, Å	*N*	*r*, Å	*σ*, Å
Gd−(O_1)	5.1 ± 0.6	2.34 ± 0.02	0.074 ± 0.011	6.1 ± 0.9	2.33 ± 0.02	0.084 ± 0.013
Gd−(O_2)	5.4 ± 0.7	2.49 ± 0.02	0.071 ± 0.011	5.4 ± 0.7	2.48 ± 0.02	0.074 ± 0.011
Gd−(N_1)	3.4 ± 0.5	2.70 ± 0.03	0.067 ± 0.010	3.4 ± 0.5	2.70 ± 0.03	0.063 ± 0.009

[c] Coordination number *N*, absorber-backscatterer distance *r*, and Debye−Waller factor *σ* with calculated standard deviations. The letters in parentheses refer to the Gd−DTPA complexes (see Figure 5) and indicate the molecule where the backscattering atom is located.

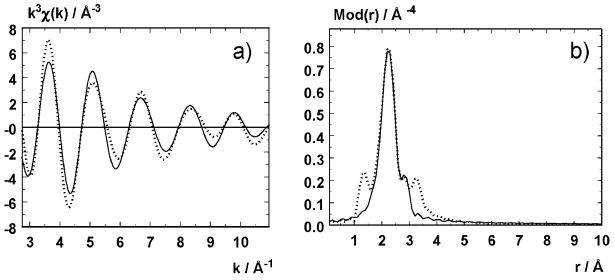

Figure 8. Experimental (dotted line) and calculated (solid line) $k^3\chi$ (k) functions (a) (k range: 2.74−10.96 Å^{-1}) and their Fourier transforms (b) for the free Gd−DTPA complex (Gd L_3-edge) (see Table 2 for fit parameter).

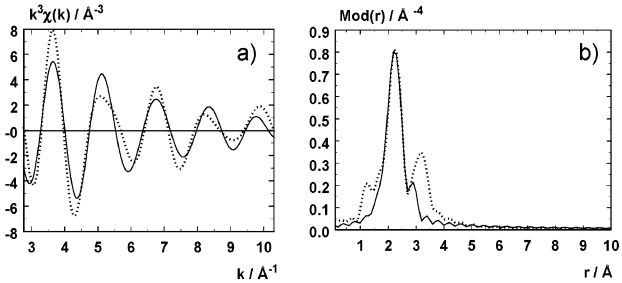

Figure 9. Experimental (dotted line) and calculated (solid line) $k^3\chi$ (k) functions (a) (k range: 3.18−11.97 Å^{-1}) and their Fourier transforms (b) for the immobilized Gd−DTPA complex (Gd L_3-edge) (see Table 2 for fit parameter).

shown. The increase of signal intensity shown in the signal-to-noise ratio of each individual carbon atom is dependent upon its spin−lattice relaxation time and its residence time within the premagnetization volume. To illustrate this concept, three of the carbon atoms in the cholesterol acetate will be discussed, namely, C-9, C-5, and C-26.

The signal of the carbon atom C-9, located at 49.9 ppm, displays a signal-to-noise ratio increase with each elevated flow rate. The signal intensity increased a total of 67% from 1 to 20 mL/min flow rate. The continuous increase of the signal intensity can be attributed to the low spin−lattice relaxation values of C-9, where T_1 is on the order of 0.4 s. This relatively short

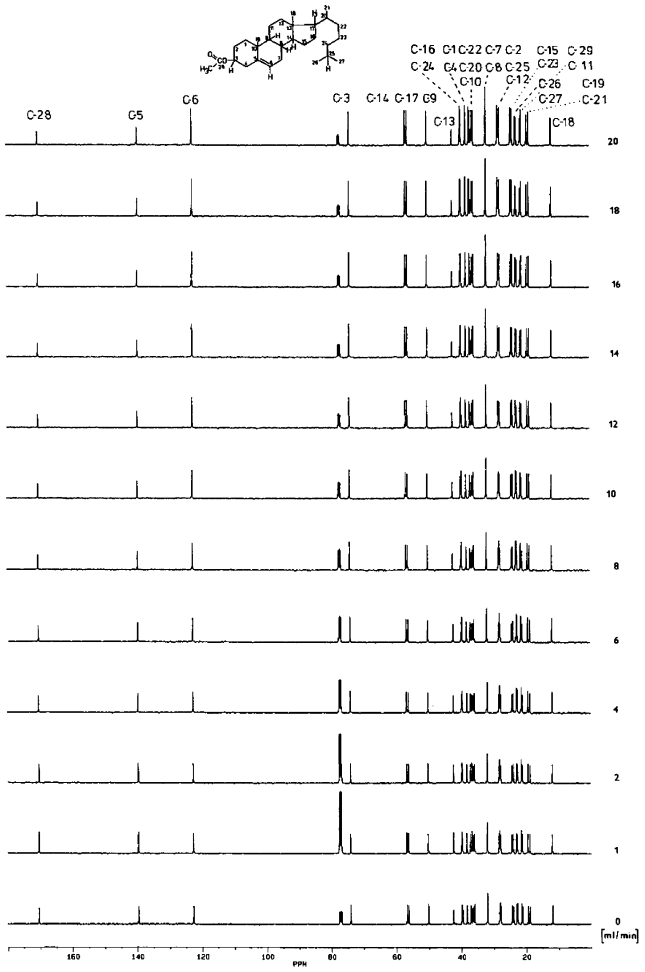

Figure 10. ^{13}C NMR spectra (100 MHz) of cholesterol acetate under *stopped*- and continuous-flow conditions.

relaxation time allows all C-9 nuclei within the solution to become fully premagnetized, even at higher flow rates. The previously mentioned premagnetization requirement, $\tau = 5T_{1(C-9)} \approx 2.0$ s, is met at each flow rate for this carbon atom. This carbon atom best demonstrates the benefits of continuous-flow ^{13}C NMR with premagnetization at higher flow rates.

In contrast to C-9, the carbon atom C-5, located at 139.5 ppm, shows a 16% decrease in the signal-to-noise ratio when the flow rate is increased from 1 to 20 mL/min. The signal intensity decrease can be attributed to the long T_1 value of this quaternary atom, $T_1 > 10$ s.

Clearly, the requirement for full pre-magnetization can only be fulfilled at the lowest flow rate of 1 mL/min for this particular nucleus. The minimum necessary residence time for the full premagnetization of C-5 is over 50 s and the longest residence time that occurred during the continuous-flow tests was 60 s at 1 mL/min. At higher flow rates, the Boltzmann distribution for this carbon atom was not achieved prior to its entrance into the detection chamber, and therefore, a lower signal intensity has resulted.

Finally, the carbon atom C-26, located at 22.8 ppm, is a nucleus with an intermediate T_1 value on the order of 2.0 s. A 33.3% increase in signal intensity can be observed between the spectra recorded at 1 and 6 mL/min. A further increase in signal-to-noise ratio does not occur at flow rates higher than 8 mL/min. At a flow rate of 6 mL/min or lower, the residence time of the nucleus within the premagnetization area is sufficient for establishing Boltzmann distribution prior to detection. The

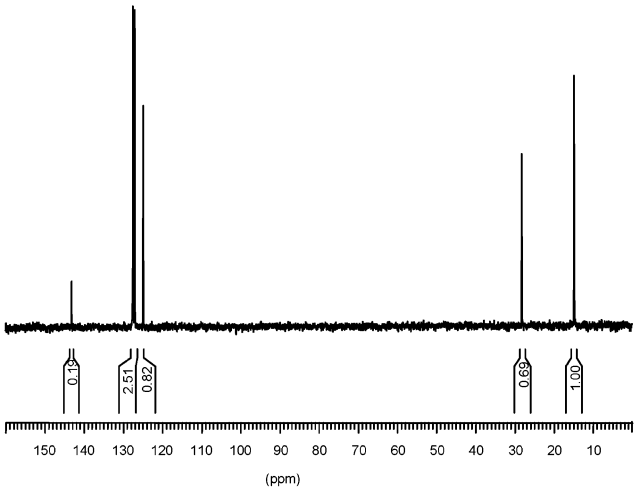

Figure 11. ^{13}C NMR spectrum of ethylbenzene with the dummy column, 10 m/min flow rate.

residence time at a flow rate of 8 mL/min or higher falls below the necessary level, $\tau = 5T_1$. To reap the full benefits of the premagnetization method for carbon atoms with intermediate T_1 values in an experiment similar to this one, the premagnetization volume could be increased.

The increase in signal-to-noise ratio was not the only observable benefit with continuous-flow ^{13}C NMR using the premagnetization method. A substantial decrease in the total acquisition time for a spectrum, was also revealed. At a flow rate of 1 mL/min, a time of 1448 s was necessary to record one spectrum, whereas at a flow rate of 20 mL/min, the corresponding total acquisition time was only 72 s. In other words, a spectrum could be recorded 20 times faster at a flow rate of 20 mL/min than at 1 mL/min. The potential benefits of the premagnetization method in conjunction with continuous-flow ^{13}C NMR are clear: there is a substantial decrease in total acquisition time and a simultaneous increase in signal-to-noise ratio. Nevertheless, quantitative NMR spectra are not achieved.

Figure 11 shows the inverse-gated decoupled ^{13}C NMR spectrum of ethylbenzene without the influence of IFRs at a flow rate of 10 mL/min; only the dummy column was used.

The integral values illustrate the problem of on-line continuous-flow ^{13}C NMR spectroscopy. The integral value with 0.19 for the quaternary carbon atom relative to the methyl group is very low. Nuclei with long T_1 relaxation times, such as quaternary and aromatic ^{13}C atoms, respectively, are underrepresented in continuous-flow ^{13}C NMR spectra. Here, a quantification is not possible.

In Figure 12, the ^{13}C NMR spectrum of ethylbenzene is depicted. The same acquisitions parameters were used like for the spectrum in Figure 11, except that Gd−DOTA was brought into the flow path of the analyte. With an integral value of 0.74, the intensity of the quaternary carbon atom is clearly increased, caused by the dramatic decrease of the T_1 time through the paramagnetic relaxation agent.

It can be clearly seen that the signal-to-noise ratio is much better in Figure 12 than that in Figure 11. Comparing the intensities of the spectrum in Figure 12 to the spectrum in Figure 11, the integral of the methyl group is increased by 14%. The reason for this increase is that, at the high flow rate of 10 mL/min, the residual time of the analyte in the magnetic field prior detection is smaller than $5T_1$, so that, in the case of the continuous-flow experiment, the Boltzmann distribution cannot be fully achieved. The use of paramagnetic relaxation agents

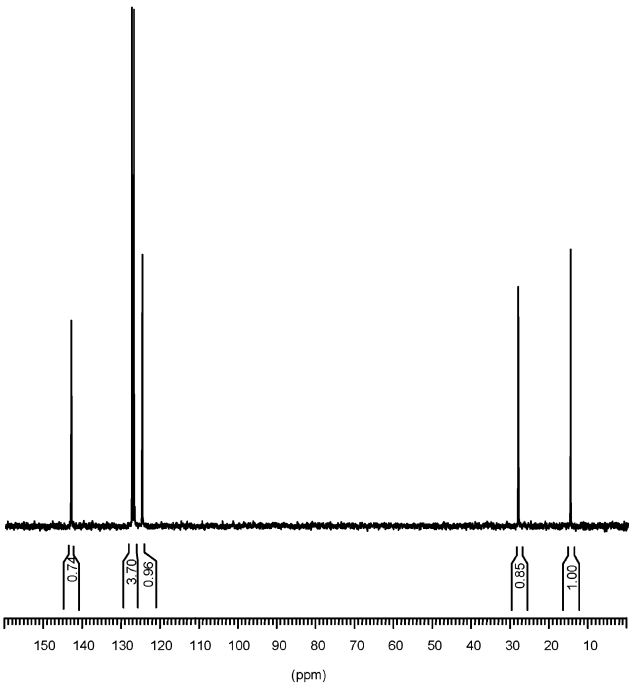

Figure 12. ^{13}C NMR spectrum of ethylbenzene with Gd−DOTA, 10 mL/min flow rate.

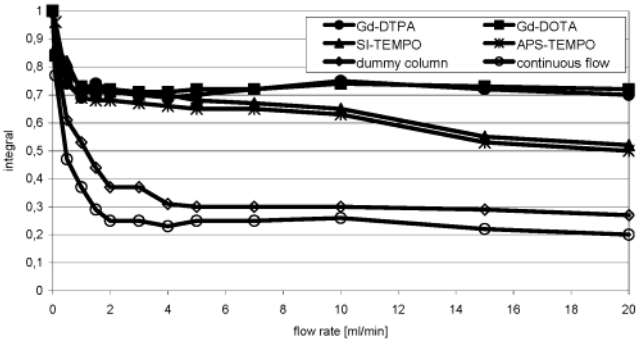

Figure 13. Dependence of the integral values of the quaternary carbon atom of ethylbenzene (referenced to the methyl carbon atom of each spectrum) from the type of used column versus flow rate.

shortens the effective T_1 times so that more *z*-magnetization can be built up.

Figure 13 compares the two SPINs, Gd−DOTA, Gd−DTPA and dummy column with conventional continuous-flow NMR measurements by applying the integral values of the quaternary ^{13}C atoms (referenced to the methyl group of each spectrum) versus the flow rate of the analyte.

By using the conventional continuous-flow method the integral value decreases dramatically with increasing flow rate and the possibility for quantification gets lost.

In the same way, the use of the dummy column, synonymous to a bigger premagnetization volume, is not sufficient for the quantification.

The influence of IFRs or paramagnetic relaxation agents on the integral values for the quaternary carbon yields only in a small decrease. Hereby, SI−TEMPO and APS−TEMPO show a similar behavior. However, both Gd(III) complexes are able to provide good quantification even at high flow rates. Therefore, the Gd−DOTA complex as well as the Gd−DTPA complex have the best properties regarding the paramagnetic relaxation effect. This was predictable by the large line width in the EPR spectra.

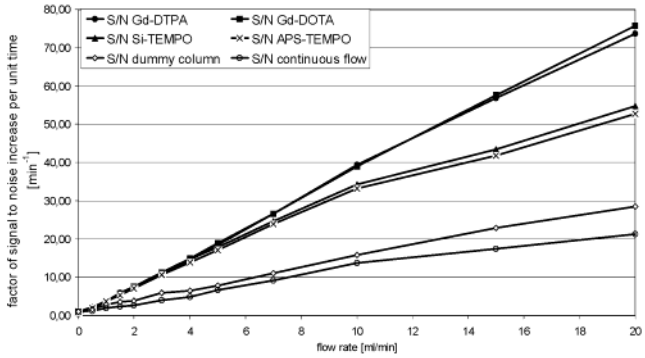

Figure 14. Factor of signal-to-noise increase per unit time in dependence from type of used column versus flow rate.

Compared to conventional flow experiments, the usage of immobilized paramagnetic relaxation agents leads to a strong increase in signal-to-noise ratio per unit time. The diagram in Figure 14 shows the factors for signal-to-noise increase per unit time (which is minute) in dependence from the type of used column (with and without paramagnetic relaxation agents) versus employed flow rate. The values are based and referenced each time on the methyl group of the respective spectrum. Indentical to the experiment with cholesterol acetate, the increase of the flow rate up to 20 mL/min leads to an increase in signal-to-noise ratio by a factor of 21. While using the dummy column, this value can be increased up to 28 at a flow rate of 20 mL/min. By using the SPINs and Gd(III) complexes, the signal-to-noise ratio at a flow rate of 20 mL/min can be increased by a factor of 55 and 75, respectively, compared to that of a static NMR spectrum. Over the whole flow range the signal-to-noise ratio is always 3−4 times higher while using the SPINs and Gd(III) complexes than that without these relaxation agents. This also means that the spectra can be recorded 3−4 times faster with immobilized paramagnetic relaxation agents over the whole flow range.

Conclusion and Outlook

It was shown that the sensitivity of continuous-flow ^{13}C NMR experiments can be increased by rising the flow, but this method is not capable of obtaining quantitative NMR spectra.

However, the application of IFRs and Gd(III) complexes in continuous-flow ^{13}C NMR spectroscopy leads to better integratable ^{13}C NMR spectra.

The signal-to-noise ratio is increased by a factor up to 75 by using the paramagnetic Gd(III) complexes and an employed flow rate of 20 mL/min. Compared to static NMR spectra, this method of paramagnetic relaxation agents together with an employed flow rate of 20 mL/min allows 75 times faster acquisition of spectra with the same quality.

With these paramagnetic relaxation agents, SPINs and especially immobilized Gd(III) complexes, a new step to quantitative continuous-flow ^{13}C NMR spectra in structure elucidation, regarding HPLC NMR coupling, is made.

The development of new capillary NMR probes, together with packed capillaries for chromatographic separation, is a promising technique. A mixed mode phase combining a separation phase with IFRs can be positioned directly before the detection cell, thereby eliminating relaxation effects in the transfer line from paramagnetic relaxation agent column to the detection cell.

In addition, with the miniaturization of the radio frequency coil, an increase in resolution and gain in sensitivity can be expected.

Acknowledgment. The excellent technical assistance of Mr. Werner Behrend in the synthesis of the immobilized paramagnetic relaxation agents is gratefully acknowledged. The authors express their appreciation to Dr. Harry C. Dorn and Dr. James. L. Sudmeier for discussion. Special thanks to Bischoff Chromatography (Leonberg, Germany) for donation of the ProntoSIL silica and to the "Deutsche Forschungsgemeinschaft" DFG and the Graduate College "Chemistry in Interphases" for support.

References and Notes

(1) Albert, K. *J. Chromatogr. A* **1999**, *199*, 856.
(2) Dorn, H. C. *Anal. Chem.* **1984**, *56*, 747.
(3) Fyfe, C. A.; Cocivera, M.; Damji, S. W. H. *Acc. Chem. Res.* **1978**, *11*, 277.
(4) Albert, K.; Dreher, E.-L.; Straub, H.; Rieker, A. *Magn. Reson. Chem.* **1987**, *25*, 919.
(5) Albert, K.; Kruppa, G.; Zeller, K.-P.; Bayer, E. *Z. Naturforsch.* **1984**, *39*, 859.
(6) LaMar, G. N. *J. Am. Chem. Soc.* **1971**, *93*, 1040.
(7) Hawkes, G. E.; Herwig, K.; Roberts, J. D. *J. Org. Chem.* **1974**, *39*, 1017.
(8) Leibfritz, D.; Roberts, J. D. *J. Am. Chem. Soc.* **1973**, *95*, 4996.
(9) Martin, L. L.; Chang, C.-J.; Floss, H. G.; Mabe, J. A.; Hagaman, E. W.; Wenkert, E. *J. Am. Chem. Soc.* **1972**, *94*, 8942.
(10) Tanabe, F. M.; Suzuki, K. T.; Jankowski, W. C. *Tetrahedron Lett.* **1973**, 4723.
(11) Levy, G. C.; Edlund, U. *J. Am. Chem. Soc.* **1975**, *97*, 4482.
(12) Shoolery, J. N. *Prog. NMR Spectrosc.* **1977**, *11*, 79.
(13) Freeman, R.; Hill, H. D. W.; Kaptein, R. *J. Magn. Reson.* **1972**, *7*, 327.
(14) Forsyth, D. A.; Hediger, M.; Mahmoud, S. S.; Glessen, B. C. *Anal. Chem.* **1982**, *54*, 1896.
(15) Cookson, D. J.; Smith, B. E. *J. Magn. Reson.* **1984**, *57*, 355.
(16) Laude, Jr. D. A.; Lee, R. W. K. Wilkins, C. L. *J. Magn. Reson.* **1984**, *60*, 453.
(17) Laude, Jr. D. A.; Lee, R. W. K. Wilkins, C. L. *Anal. Chem.* **1985**, *57*, 1286.
(18) Albert, K.; Nieder, M.; Bayer, E. *J. Chromatogr.* **1985**, *346*, 17.
(19) Bayer, E.; Albert, K. *J. Chromatogr.* **1984**, *312*, 91.
(20) Bruck, D.; Dudley, R.; Fyfe, C. A.; Van Delden, J. *J. Magn. Reson.* **1981**, *42*, 51.
(21) Laude, Jr. D. A.; Lee, R. W. K. Wilkins, C. L. *Anal. Chem.* **1985**, *57*, 1286.
(22) Zhang, Y.; Laude, Jr. D. A. *J. Magn. Reson.* **1990**, *87*, 46.
(23) Lauffer, R. B. *Chem. Rev.* **1987**, *87*, 901.
(24) Weinmann, H.-J.; Mühler, A.; Radüchel, B. In *Encyclopedia of Nuclear Magnetic Resonance*; John Wiley and Sons Ltd: New York, 1996; p 2166.
(25) Caravan, P.; Ellison, J. J.; McMurry, T. J.; Lauffer, R. B. *Chem. Rev.* **1999**, *99*, 2293.
(26) Clarkson, R. B, Smirnov, A. I.; Smirnova, T. I.; Kang, H.; Belford, R. L.; Earle, K.; Freed, J. H. *Mol. Phys.* **1998**, *95(6)*, 1325.
(27) Aime, S.; Botta, M.; Ermondi, G. *Inorg. Chem.* **1992**, *31*, 4291.
(28) Szilágyi, E.; Tóth, E.; Brücher, E.; Merbach, A. E. *J. Chem. Soc., Dalton Trans.* **1999**, 2481.
(29) Aime, S.; Barge, A.; Bruce, J. I.; Botta, M.; Howard, J. A. K.; Moloney, J. M.; Parker, D.; de Sousa, A. S.; Woods, M. *J. Am. Chem. Soc.* **1999**, *121*, 5762.
(30) Stern, E. A. *Phys. Rev. B* **1974**, *10*, 3027.
(31) Lytle, F. W.; Sayers, D. E.; Stern, E. A. *Phys. Rev. B*, **1975**, *11*, 4825.
(32) Sudmeier, J.; Günther, U.; Albert, K.; Bachovchin, W. *J. Magn. Reson A* **1996**, *118*, 145.
(33) Günther, U.; Sudmeier, J. L.; Albert, K.; Bachovchin, W. W. *J. Magn. Res.* **1995**, *117*, 73.
(34) Gitti, R.; Wild, C.; Tsiao, C.; Zimmer, K.; Glass, T. E.; Dorn, H. C. *J. Am. Chem. Soc.* **1988**, *110*, 2294.
(35) Dorn, H. C.; Wang, J.; Allen, L.; Sweeney, D.; Glass, T. E. *J. Magn. Res.* **1988**, *79*, 404.
(36) Dorn, H. C.; Gitti, R.; Tsai, K. H.; Glass, T. E. *Chem. Phys. Lett.* **1989**, *155*, 227.
(37) Dorn, H. C.; Gu, J.; Bethune, D. S.; Johnson, R. D.; Yannoni, C. S. *Chem. Phys. Lett.* **1993**, *203*, 549.
(38) Dorn, H. C.; Glass, T. E.; Gitti, R.; Tsai, K. H. *Appl. Magn. Reson.* **1991**, *2*, 9.
(39) Stevenson, S.; Glass, T.; Dorn, H. C. *Anal. Chem.* **1998**, *70*, 2623.
(40) Stevenson, S.; Dorn, H. C. *Anal. Chem.* **1994**, *66*, 2993.
(41) Gitti, R.; Wild, C.; Tsiao, C.; Zimmer, K.; Glass, T. E.; Dorn, H. C. *J. Am. Chem. Soc.* **1988**, *110*, 2294.
(42) Müller-Warmuth, W.; Meise-Gresch, K. *Adv. Magn. Res.* **1983**, *11*, 1.
(43) Buszewski, B. *Chromatographia* **1992**, *34*, 573.
(44) Ertel, T. S.; Bertagnolli, H.; Hückmann, S.; Kolb, U.; Peter, D. *Appl. Spectrosc.* **1992**, *46*, 690.
(45) Newville, M.; Livins, P.; Yakobi, Y.; Rehr, J. J.; Stern, E. A. *Phys. Rev. B* **1993**, *47*, 14126.
(46) Gurman, S. J.; Binsted, N.; Ross, I. *J. Phys. C* **1986**, *19*, 1845.
(47) Dubost, J.-P.; Leger, J.-M.; Langlois, M.-H.; Meyer, D.; Schaefer, M. *C. R. Acad. Sci. Paris, Ser. II* **1991**, *t. 312*, 349−354.
(48) Bénazeth, S.; Purans, J.; Chalbot, M.-C.; Nguyen-van Duong, M. K.; Nicolas, L.; Keller, F.; Gaudemer, A. *Inorg. Chem.* **1998**, *37*, 3667−3674.